

Conditional Hybrid Nonclassicality

E. Agudelo,^{1,*} J. Sperling,² L. S. Costanzo,^{3,4} M. Bellini,^{3,4} A. Zavatta,^{3,4} and W. Vogel¹

¹*AG Theoretische Quantenoptik, Institut für Physik, Universität Rostock, D-18051 Rostock, Germany*

²*Clarendon Laboratory, University of Oxford, Parks Road, Oxford OX1 3PU, United Kingdom*

³*Istituto Nazionale di Ottica (INO-CNR), Largo Enrico Fermi 6, 50125 Florence, Italy*

⁴*LENS and Department of Physics, University of Firenze, 50019 Sesto Fiorentino, Florence, Italy*

(Dated: February 15, 2017)

We provide a general method to characterize the nonclassicality in compound discrete- and continuous-variable systems. For this purpose, we introduce the operational notion of conditional hybrid nonclassicality which relates to the ability to produce a nonclassical continuous-variable state by projecting onto a general superposition of discrete-variable states. We discuss the importance of this form of quantumness in connection with interfaces for quantum communication. To verify the conditional hybrid nonclassicality, a matrix version of a nonclassicality quasiprobability is derived. We experimentally generate an entangled hybrid Schrödinger cat state, using a coherent photon-addition process acting on two temporal modes, and we directly sample its nonclassicality quasiprobability matrix. The considered types of quantum effects are certified with high statistical significance.

Introduction.— The investigation of signatures of nonclassicality is of crucial importance for the understanding, engineering, and controlling of quantum systems. The knowledge of various forms of quantumness plays a central role in modern research, ranging from fundamental tests of quantum physics [1, 2] to applications close to commercial quantum information processing [3–5]. Especially for secure communication, quantum correlations of light have been vastly exploited [6]. To apply quantum enhanced communication protocols, it is indispensable to characterize the correlations between different systems. In particular, the interface between continuous-variable (CV) and discrete-variable (DV) systems has to be understood for implementing quantum communication on a highly variable basis and for employing the benefits of both kinds of systems [7].

In CV quantum optics, the standard concept of nonclassicality is based on the impossibility of describing field correlations in terms of classical electrodynamics. This notion defines nonclassical light in terms of a Glauber-Sudarshan P representation [8–10] that does not resemble a classical probability distribution. Thus, quasiprobability representations are a direct and intuitive way to discern classical from quantum field theories. Moreover, the negativities of these quasiprobabilities have been closely related to other nonclassicality features, like contextuality [11, 12] and to symmetries of the quantum state [13].

However, the P distribution can be strongly singular for many physical states [14]. Different regularization strategies have been investigated in order to use the advantages of the P representation. For instance, s -parametrized quasiprobabilities [15, 16] have been introduced, which include the Wigner function for $s = 0$. But the s parameter not only regularizes the singularities, it also limits the sensitivity to verify quantumness.

To overcome this deficiency, non-Gaussian nonclassicality filters have been applied to uncover all forms of single- and multimode nonclassicality in terms of regular nonclassicality quasiprobabilities [17, 18].

The DV regime of quantum optics can be, for example, related to the particle picture of quantized fields using the Fock representation of states. This expansion in terms of photon number states also allows for a complete characterization of light fields [19]. Other realizations of such so-called photonic qudits are based on the angular momentum of light [20, 21]. The advantage of this representation is clearly its direct connection to quantum information processing, which is formulated in qudits as the basic carriers of information.

Traditionally, the CV and DV representation of light have been individually exploited, but the connection between these two complementary regimes has not been extensively studied. One of the few relations between CD and DV systems that has been established is based on the observation that qubits can be constructed out of CV states [22, 23]. Another early attempt to consider a hybrid system was elaborated to measure nonclassicality between a vibrational mode and the electronic states of a trapped two-level atom based on a Wigner matrix [24]. More recently, the experimental generation of hybrid entanglement was reported [27, 28] and its entanglement had been investigated [29]. Even though quantum-correlated hybrid systems are of high interest for quantum information processing [30, 31], a universal way to access their nonclassicality is missing yet.

In this Letter, we introduce and implement a method for describing and identifying nonclassicality in hybrid, i.e., correlated DV and CV, systems of light. The operational meaning of the resulting notion of conditional hybrid nonclassicality (CHN) is motivated. This concept of quantumness is shown to be experimentally accessible via a nonclassicality quasiprobability (NQP) matrix. We apply our technique to an experimentally generated hybrid entangled Schrödinger cat state to characterize its

* elizabeth.ospina@uni-rostock.de

quantum features with high significance.

Conditional hybrid nonclassicality.— For motivating our notion of CHN, we firstly consider an application which, eventually, yields our general concept. Suppose, we have an entangled Schrödinger cat state,

$$|\Psi_{\text{cat}}\rangle = 2^{-1/2}(|\beta\rangle \otimes |0\rangle + |-\beta\rangle \otimes |1\rangle). \quad (1)$$

The first subsystem is given in a CV description of coherent states. For the second subsystem, we have a DV expansion in terms of Fock states. The implementation of $|\Psi_{\text{cat}}\rangle$ was established through tailoring the correlation between $|\pm\beta\rangle$ and $|0\rangle, |1\rangle$ [25–27, 32, 33].

For establishing a DV-CV communication node, we aim at transferring the information of a qubit $|q\rangle = q_0|0\rangle + q_1|1\rangle$ (a third subsystem) into a CV encoding via the state (1). This can be achieved by performing a joint projection of the composed state $|\Psi_{\text{cat}}\rangle \otimes |q\rangle$ onto the Bell state $|\phi^+\rangle = 2^{-1/2}(|0\rangle \otimes |0\rangle + |1\rangle \otimes |1\rangle)$ in the second and third mode as it is done in quantum teleportation protocols [34]. Hence, we get analogously

$$|\Psi_q\rangle = \mathcal{N}(q_0|\beta\rangle + q_1|-\beta\rangle), \quad (2)$$

where \mathcal{N} is a proper normalization constant. The state (2) now carries the information of the qubit $|q\rangle$. If the qubit represents a classical truth value, $|q\rangle \in \{|0\rangle, |1\rangle\}$, we also get a classical coherent state $|\pm\beta\rangle$ in the resulting CV state (2). Yet, any superposition state $|q\rangle$ will also result in a nonclassical superposition state $|\Psi_q\rangle$. In other words, the hybrid state (1) has the potential to yield a nonclassical CV state through DV projections.

Let us abstract the above observation. Suppose $\hat{\rho}$ is a CV-DV-hybrid state and $\hat{\Pi}$ is a non-negative operator in the DV subsystem. Without loss of generality we can restrict ourselves to rank-one operators $\hat{\Pi} = |\psi\rangle\langle\psi|$, with $|\psi\rangle = \sum_{m=0}^{\infty} \psi_m |m\rangle$, because any other non-negative operator can be considered as a positive linear combination of such projectors. Now, the conditional CV state is defined in terms of the partial projection

$$\hat{\rho}_{|\hat{\Pi}} = \mathcal{N} \text{tr}_{\text{DV}}(\hat{\rho}[\hat{1} \otimes \hat{\Pi}]) = \int d^2\alpha P(\alpha|\hat{\Pi})|\alpha\rangle\langle\alpha|, \quad (3)$$

where \mathcal{N} is a normalization constant and $P(\alpha|\hat{\Pi})$ is the conditional Glauber-Sudarshan distribution. We can now extend the concept of single-mode CV nonclassicality [10] to our operationally defined notion of CHN: *The CV-DV hybrid state $\hat{\rho}$ shows CHN if there exists a DV projection $\hat{\Pi}$ such that $P(\alpha|\hat{\Pi})$ is not a classical probability distribution.*

Especially, this definition applies to the previously considered example of the entangled Schrödinger cat state (1). Moreover, this definition extends the initial idea to mixed states and to generalizations of DV systems beyond a two-level qubit. For example, a CV-qudit hybrid state $|\Psi\rangle = \sum_{m=0}^{d-1} c_m |\beta_m\rangle \otimes |m\rangle$ clearly exhibits CHN (for non-trivial coefficients c_m). From the operational point of view, our notion of quantumness can be also

interpreted in terms of the heralded generation of quantum states. That is, CHN of a state ensures that there exists a projection of the DV mode which results in the realization of a CV nonclassical state. Also note that another form of conditional nonclassicality has been recently studied in the context of photon statistics [35]

Nonclassicality quasiprobability matrix.— Our notion of CHN requires to explore all possible projections $\hat{\Pi} = |\psi\rangle\langle\psi|$. For one of them, the nonclassicality has to be verified from the conditional and possibly highly singular Glauber-Sudarshan distribution $P(\alpha|\hat{\Pi})$. To overcome these difficulties, we now formulate a directly accessible and equivalent method.

Using the concept of the P representation, one can expand any mixed, hybrid state $\hat{\rho}$ in the form

$$\hat{\rho} = \int d^2\alpha \sum_{m,n=0}^{\infty} P_{m,n}(\alpha) |\alpha\rangle\langle\alpha| \otimes |m\rangle\langle n|. \quad (4)$$

Note that $P_{m,n}(\alpha)$ can be a complex-valued function for $m \neq n$. Moreover, the function fulfills the properties of normalization, $\text{tr}(\hat{\rho}) = \int d^2\alpha \sum_n P_{n,n}(\alpha) = 1$, and symmetry, $\hat{\rho} = \hat{\rho}^\dagger$ implies $P_{m,n}(\alpha) = P_{n,m}^*(\alpha)$, which are necessary for the proper representation of the physical state $\hat{\rho}$. Now, the P distribution conditioned onto the DV state $|\psi\rangle = \sum_{m=0}^{\infty} \psi_m |m\rangle$ can be written in the form

$$P(\alpha|\hat{\Pi}) = \mathcal{N} \vec{\psi}^\dagger \mathbf{P}(\alpha) \vec{\psi}, \quad (5)$$

where $\mathbf{P}(\alpha) = (P_{m,n}(\alpha))_{m,n}$ and the projection state vector $\vec{\psi} = (\psi_n)_n$. As the normalization constant \mathcal{N} is positive, we get from Eq. (5) that $P(\alpha|\hat{\Pi})$ is a classical (non-negative) probability distribution for any projection iff the P matrix is non-negative, $\mathbf{P}(\alpha) \geq 0$ for all α . Note that a restriction to a 2×2 matrix and a convolution with Gaussian noise of $\mathbf{P}(\alpha)$ yields the Wigner matrix approach of Ref. [24].

As the P function can be highly singular [14], the matrix $\mathbf{P}(\alpha)$ can be irregular as well. For a single CV mode, a nonclassicality-preserving regularization process has been proposed which consists of a convolution of the original P function with a suitable, non-Gaussian kernel $\tilde{\Omega}(\alpha)$ [17]. For our purposes, this approach can be generalized, yielding directly to the NQP matrix, $\mathbf{P}_\Omega(\alpha) = (P_{\Omega;m,n}(\alpha))_{m,n}$ with the regular matrix elements

$$P_{\Omega;m,n}(\alpha) = \int d^2\alpha' \tilde{\Omega}_w(\alpha - \alpha') P_{m,n}(\alpha'), \quad (6)$$

where our choice of a kernel $\tilde{\Omega}_w(\alpha)$ is the Fourier transformation of the autocorrelation function $\Omega_w(\gamma) = \mathcal{N}_w \int d^2\gamma' e^{-(|\gamma'|/w)^4} e^{-(|\gamma+\gamma'|/w)^4}$ with a normalization constant \mathcal{N}_w , such that $\Omega_w(0) = 1$, and $w > 0$ denoting the filter width [17, 36, 37]. In the limit $w \rightarrow \infty$, we recover the original $\mathbf{P}(\alpha)$.

Now, the CHN can be identified with the following necessary and sufficient condition: *The state $\hat{\rho}$ shows CHN*

iff there exists $w > 0$ and $\alpha \in \mathbb{C}$ such that the NQP matrix $\mathbf{P}_\Omega(\alpha)$ is not positive-semidefinite,

$$\mathbf{P}_\Omega(\alpha) \not\geq 0. \quad (7)$$

We will also use the equivalence of this condition (7) with the existence of a negative eigenvalue of $\mathbf{P}_\Omega(\alpha)$.

To experimentally apply condition (7), we reconstruct the NQP matrix with so-call pattern functions [38, 39]. Our data are recorded using balanced homodyne detection, which has been used for optical state tomography [19, 40], detector tomography [41], tomography in atomic physics [42, 43], and optomechanics [44]. The reconstruction of a DV density matrix in the Fock basis via balanced homodyne detection is well known [45–47] and their pattern functions are labeled as $F_{m,n}(x', \varphi')$, where x' is the quadrature for the phase φ' . In the CV scenario, pattern functions $f_\Omega(\alpha, w; x, \varphi)$ for the regularized quasiprobabilities P_Ω have been introduced and applied [36, 37, 48]. We can combine the approaches for CV and DV systems, in order to sample the elements of the NQP matrix $\mathbf{P}_\Omega(\alpha)$ from the measured quadratures data points $\{(x_j, \varphi_j, x'_j, \varphi'_j)\}_{j=1}^N$,

$$P_{\Omega;m,n}(\alpha) = \sum_{j=1}^N \varpi_j f_\Omega(\alpha, w; x_j, \varphi_j) F_{m,n}(x'_j, \varphi'_j), \quad (8)$$

with weights $\varpi_j \geq 0$ and $\sum_j \varpi_j = 1$. The full treatment of this sampling approach can be found in the Supplemental Material [49] together with a derivation of the weights and the sampling error $\sigma(P_{\Omega;m,n}(\alpha))$. The introduction of a weighted mean becomes essential as we have data sets which are not uniformly distributed in phase. The weighting corrects for this unbalanced distribution of data points, which extends the applicability of our method beyond previous approaches.

Experimental implementation.— In Fig. 1, we outline the experiment to produce a state of the type (1). A detailed analysis of the setup may be found in Ref. [27]. In this experiment, a single photon-addition device (labeled as \hat{a}^\dagger) is fed with two distinct temporal modes containing, respectively, a coherent and a vacuum state, $|\beta\rangle \otimes |0\rangle$. The device realizes a stimulated parametric down-conversion process heralded by the detection of a idler photon; see [50] for a detailed theoretical description. A properly unbalanced Mach-Zehnder interferometer is placed in the idler path so as to restore indistinguishability between the temporal modes that originated the herald photon.

A click of one of the detectors after the interferometer certifies the addition of a photon in either of the modes, $t\hat{a}^\dagger \otimes \hat{1} + r\hat{1} \otimes \hat{a}^\dagger$. This superpositions of creation operations is parametrized with t ($r = \sqrt{1 - |t|^2}$), which can be controlled via the relative transmission between the two interferometer arms. Choosing $t = 1/\sqrt{|\beta|^2 + 2}$

results in correlated signal pulses of the form

$$\begin{aligned} |\Psi'\rangle &= 2^{-1/2} \left(|\beta\rangle \otimes |1\rangle + \frac{\hat{a}^\dagger |\beta\rangle}{\sqrt{\langle \beta | \hat{a} \hat{a}^\dagger | \beta \rangle}} \otimes |0\rangle \right) \\ &\approx 2^{-1/2} (|\beta\rangle \otimes |1\rangle + |g\beta\rangle \otimes |0\rangle). \end{aligned} \quad (9)$$

Here the approximation $\hat{a}^\dagger |\beta\rangle \approx |g\beta\rangle$ is used, where the optimal amplitude gain (maximizing the fidelity) is $g = (1 + \sqrt{1 + 4/|\beta|^2})/2$.

The symmetric target state (1) can be simply obtained with a phase-space displacement, as in Ref. [27]. However, since here we just focus on the hybrid nonclassical correlations that are not affected by such a displacement operation, the experimental state (9) with $\beta \simeq 1.4$ is analyzed instead.

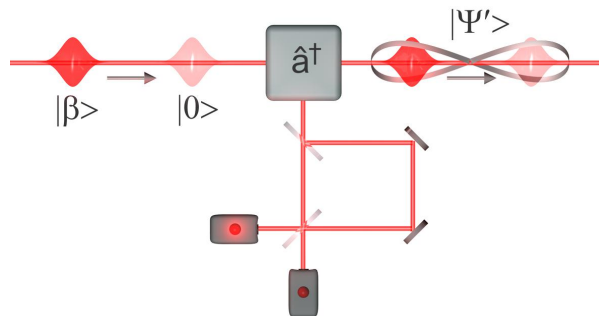


FIG. 1. (Color online) Experimental scheme for the generation of a correlated hybrid state.

Results.— The balanced homodyne detection of the generated state yields an ensemble $\{(x_j, \varphi_j, x'_j, \varphi'_j)\}_{j=1}^N$ of $N = 372\,000$ data points of quadrature values. Based on our sampling approach in Eq. (8), we reconstructed the elements of the NQP matrix $\mathbf{P}_\Omega(\alpha)$ which are shown in Fig. 2. For the DV part, we present the first three elements, $m, n \in \{0, 1, 2\}$. Higher contributions are not relevant as they have a reconstruction error $\sigma(P_{\Omega;m,n}(\alpha))$ that exceeds 34%. The first observation from Fig. 2 is that the reconstruction approximates to some extent our theoretical expectations of the state (1). With our sensitive approach, however, we can also identify a number of deviations and we can test for CHN in terms of condition (7). Let us discuss some results of our analysis.

In contrast to the ideal state (1), our produced state includes non-zero matrix contributions for more than one photon in the DV mode, e.g., $P_{\Omega;2,2}(\alpha) \neq 0$. Imperfect detectors which are employed in the addition process can be one source of this [50]. The diagonal elements also exhibit negative contributions, e.g., $P_{\Omega;0,0}(\alpha) < 0$ for some α , although the projection onto the DV vacuum state is expected to correspond to a classical coherent state. More rigorously, the $|n\rangle\langle n|$ -conditioned, regularized P functions show a maximal significance of negativities of $S_0 = 8$, $S_1 = 4$, and $S_2 = 3$ standard deviations, where $S_n = \max_\alpha [-P_{\Omega;n,n}(\alpha)/\sigma(P_{\Omega;n,n}(\alpha))]$. The reason for

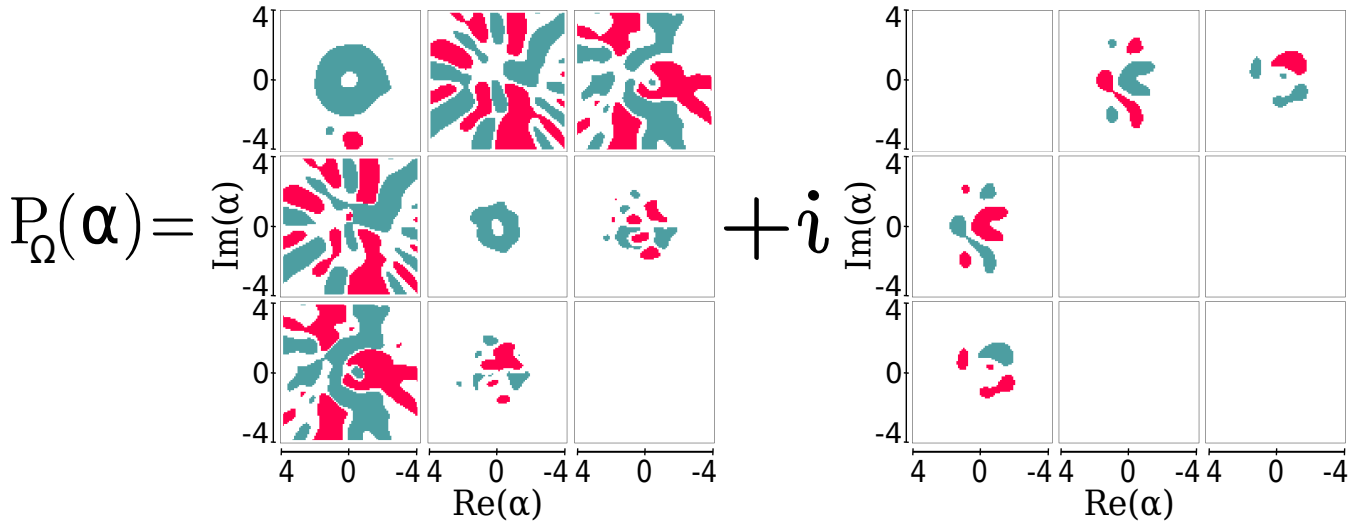


FIG. 2. (Color online) Reconstructed 3×3 NQP matrix $\mathbf{P}_\Omega(\alpha) = (P_{\Omega;m,n}(\alpha))_{m,n=0,1,2}$. Significant values, $|S| > 5$, are displayed. Green denotes positive values and red negative ones.

the significant negativities of $P_{\Omega;0,0}(\alpha)$ is that our technique is sensitive enough to go beyond the approximation $\hat{a}^\dagger|\beta\rangle \approx |g\beta\rangle$ in Eq. (9). Note, additional theoretical analysis shows that the Wigner function of $\hat{a}^\dagger|\beta\rangle$ for the realized β cannot significantly exhibit this nonclassicality (see also [27]).

So far we discussed the Fock-diagonal projections of the NQP matrix. Now, we also apply our CHN criteria (7) for general projections $\vec{\psi}$ in Eq. (5). For this purpose, we adopt the eigenvalue approach from Ref. [51] and we define the submatrices $\mathbf{P}_{\Omega;n}(\alpha) = (P_{\Omega;m,m'}(\alpha))_{m,m'=0,\dots,n}$. Hence, we have that $\mathbf{P}_{\Omega;0}(\alpha)$ corresponds to the previously considered $P_{\Omega;0,0}(\alpha)$, $\mathbf{P}_{\Omega;1}(\alpha)$ corresponds to the DV subspace in which the state (1) lives (i.e., the full span of the Fock states $|0\rangle, |1\rangle$), and $\mathbf{P}_{\Omega;2}(\alpha)$ is the full matrix shown in Fig. 2. The eigenvector $\vec{\psi}_{n,\alpha}$ to the minimal eigenvalue of $\mathbf{P}_{\Omega;n}(\alpha)$ describes the optimal projection $\hat{\Pi} = |\psi\rangle\langle\psi|$ that can be done in the n -photon subspace. This means, a negative eigenvalue $e_{n,\alpha} = \vec{\psi}_{n,\alpha}^\dagger \mathbf{P}_{\Omega;n}(\alpha) \vec{\psi}_{n,\alpha}$ certifies the maximal CHN for this point α in phase space.

From the analysis of the reconstructed NQP matrix, we computed the maximal significances of its negativities, $\Sigma_n = \max_\alpha [-e_{n,\alpha}/\sigma(e_{n,\alpha})]$, similarly to S_n for diagonal projections. As expected for the simplest case $n = 0$, we observe a CHN with $S_0 = \Sigma_0 = 8$ standard deviations. However, for $n = 1$, the off-diagonal contributions $P_{\Omega;0,1}(\alpha)$ have quite strong impact, which can be seen from the maximal verification of quantumness with $\Sigma_1 = 32$ standard deviations. For comparison, the two possible diagonal projection in this subspace yield only $S_0 = 8$ and $S_1 = 4$. Hence, the major source of CHN comes from the CV-DV interference terms $P_{\Omega;0,1}(\alpha)$, where information on the nonclassical correlations is encoded. The latter is dominated by the

coherent superpositions of the $|\beta\rangle \otimes |0\rangle$ and $|\beta\rangle \otimes |1\rangle$ terms. The negativity of the full 3×3 matrix in Fig. 2 only adds a small contribution to the nonclassicality, i.e., $\Sigma_2 = 33 \approx \Sigma_1$. In summary, our present experimental CHN data analysis of the generated state gives more insight in the fine structure of nonclassicality compared with the technique in [27].

Conclusions.— Motivated by the need of realizing interlinks between continuous and discrete variable systems for quantum communication, we formulated the notion of conditional hybrid nonclassicality. Conditional hybrid nonclassicality can be considered to be the ability of a compound CV-DV state to produce a nonclassical state when performing a projecting measurement (i.e., heralding) in one subsystem. Beyond the conceptual formulation, we derived a directly accessible technique to verify the quantumness under study in terms of a regular phase-space matrix. The latter functional matrix highlights the interplay between the continuous and discrete degrees of freedom. Similarly to scalar phase-space representations, negativities in our quasiprobability matrix certify the conditional nonclassicality. The analyzed state was implemented through correlating two temporally separated pulses of light with the help of an interferometric photon-addition process. We sampled the nonclassicality quasiprobability matrix with properly designed pattern functions and performed a detailed analysis of the state. Altogether, we demonstrated conditional hybrid nonclassicality with high statistical significance beyond the sensitivity of other nonclassicality criteria.

The notion of conditional hybrid nonclassicality is a promising candidate for characterizing the usefulness of states for applications at the interface between discrete- and continuous-variable quantum systems. Our nonclassicality quasiprobability matrices can be directly sampled from experimental data and they yield an intuitive

understanding of the quantum nature of states and correlations. Future generalizations and applications may further extend the operational meaning of our findings beyond the examples considered here.

Acknowledgement.— The authors gratefully acknowledge fruitful discussions with B. Kühn. This work was supported by the Deutsche Forschungsgemeinschaft through SFB 652, project No. B12. J. S. and W. V. acknowledge funding from the European Union’s Horizon 2020 research and innovation programme under grant agreement No 665148. L. S. C., M. B., and A. Z. acknowledge support from Ente Cassa di Risparmio di Firenze and from the Italian Ministry of Education, University and Research (MIUR), under the ‘Progetto Premiale: QSecGroundSpace’.

APPENDIX: NQP MATRIX RECONSTRUCTION

The nonclassicality quasiprobability (NQP) matrix can be directly sampled from the experimental data of our generated hybrid state. This appendix is a guide towards the proper reconstruction of their matrix elements. In a first part (Sec. A), we review some known methods and describe the modifications for the state reconstruction used here. In the second part (Sec. B), we derive a treatment for non-uniform phase distributions based on a weighted sampling approach.

Appendix A: Pattern functions

Consider the physical quantity F and the pair of variables (x, φ) , quadratures x and phases φ , that follow the quadrature probability distribution $p(x; \varphi)$, where $\int_{-\infty}^{\infty} dx p(x; \varphi) = 1$ for all φ . The x and φ values are measured in the range $-\infty < x < \infty$ and $0 \leq \varphi < \pi$, respectively. Then F can be written as

$$F = \int_{-\infty}^{\infty} dx \int_0^{\pi} d\varphi \frac{p(x, \varphi)}{\pi} f(x, \varphi), \quad (\text{A1})$$

which means that the quantity F can be determined through the pattern functions $f(x, \varphi)$. This family of such so-called pattern functions allows us to directly estimate \overline{F} (i.e., sample the quantity F) together with its standard error of the mean $\sigma(F)$ from a given experimental data set $\{(x_j, \varphi_j)\}_{j=1}^N$ via

$$\overline{F} = \frac{1}{N} \sum_{j=1}^N f(x_j, \varphi_j), \quad (\text{A2})$$

and $\sigma(F)^2 = (\overline{F^2} - \overline{F}^2)/N$ for an equally weighted sampling. Note that the denominator N in $\sigma(F)^2$ is typically replaced by $N-1$, the so-called Bessel’s correction, which becomes irrelevant for large N . In this section, the phases are assumed to be uniformly distributed. This standard sampling approach will be generalized in Sec. B.

We deal with physical quantities that can be estimated from balanced homodyne detection (BHD). This yields the quadrature variances $x(\varphi)$, where φ is an experimentally adjustable phase-difference between the signal field and the local oscillator. The set of data which is obtained from two BHDs, considering a two-mode system, consist in N pairs $\{(x_{1,j}, \varphi_{1,j}, x_{2,j}, \varphi_{2,j})\}_{j=1}^N$. In our current scenario, the data set is an ensemble of $N = 372\,000$ measured quadrature values for an equally spaced set of six fixed phase values per mode. A histogram of the measured marginal quadrature distributions for the discrete-variable (DV) mode, x_1 , and the continuous-variable (CV) mode, x_2 , is shown in Fig. 3.

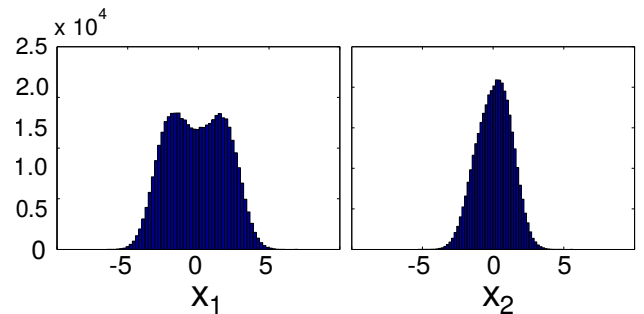


FIG. 3. The measured counts of the marginal quadrature distributions for the DV mode, x_1 , and the CV mode, x_2 . The total number of data points is $N = 372\,000$.

1. CV pattern functions

The pattern functions for a single-mode filtered NQP $P_{\Omega}(\alpha)$ have been derived in Ref. [37]. It was shown that

$$P_{\Omega}(\alpha) = \int_{-\infty}^{\infty} dx \int_0^{\pi} d\varphi \frac{p(x, \varphi)}{\pi} f_{\Omega}(x, \varphi; \alpha, w), \quad (\text{A3})$$

with the pattern function

$$f_{\Omega}(x, \varphi; \alpha, w) = \frac{1}{\pi} \int_{-\infty}^{\infty} db |b| e^{2ib|\alpha| \sin(\arg(\alpha) + \varphi - \pi/2)} e^{ibx} e^{b/2} \Omega_w(b). \quad (\text{A4})$$

Here, we restrict ourselves to the filter function $\Omega_w(\gamma) = \mathcal{N}_w \int d^2\gamma' e^{-(|\gamma'|/w)^4} e^{-(|\gamma + \gamma'|/w)^4}$, with \mathcal{N}_w being chosen such that $\Omega_w(0) = 1$ and $w > 0$ denoting the filter width. The nonclassicality quasiprobability, $P_{\Omega}(\alpha)$, is represented as the expectation value of the function $f_{\Omega}(x, \varphi; \alpha, w)$. Analogously to Eq. (A2), when the pairs (x, φ) are experimentally measured the expectation value of P_{Ω} can be replaced by the empirical estimate,

$$\overline{P_{\Omega}(\alpha)} = \frac{1}{N} \sum_{j=1}^N f_{\Omega}(x_j, \varphi_j; \alpha, w). \quad (\text{A5})$$

As a set of data for BHD includes in general a large number of data points, several hundred of thousands, the

fast evaluation of pattern functions is quite relevant. For this purpose, a Fourier technique is applied [37].

2. DV pattern functions

The reconstruction of the density matrix elements in the Fock representation, $\rho_{m,n} = \langle m | \hat{\rho} | n \rangle$, from the quadrature component distribution requires another set of pattern functions, $F_{m,n}(x, \varphi)$, which gives

$$\rho_{m,n} = \int_{-\infty}^{\infty} dx \int_0^{\pi} d\varphi \frac{p(x; \varphi)}{\pi} F_{m,n}(x, \varphi). \quad (\text{A6})$$

The approach to compute the pattern function and their explicit form can be found in Refs. [39, 52]. Decomposing $F_{k,l}(x, \varphi) = f_{k,l}(x) e^{i(k-l)\varphi}$, they are given by

$$f_{k,l}(x) = i^{k-l} \sqrt{\frac{k!}{l!}} \int_{-\infty}^{\infty} du |u| e^{-u^2/2} u^{l-k} L_k^{l-k}(u^2) e^{iux}, \quad (\text{A7})$$

where L_k^{l-k} denote the associated Laguerre polynomials. Analogously to the CV case, the expectation value can be replaced by the empirical estimate

$$\overline{\rho_{m,n}} = \frac{1}{N} \sum_{j=1}^N F_{m,n}(x_j, \varphi_j). \quad (\text{A8})$$

3. Higher-order, bipartite significances

Summarizing the CV and DV sampling approaches, we find that hybrid systems can be described through the elements of the NQP matrix, $P_{\Omega;m,n}(\alpha)$. These elements can be sampled according to

$$\overline{P_{\Omega;m,n}(\alpha)} = \frac{1}{N} \sum_{j=1}^N f_{\Omega}(x_{1,j}, \varphi_{1,j}; \alpha, w) F_{m,n}(x_{2,j}, \varphi_{2,j}). \quad (\text{A9})$$

For classical states, the NQP matrix is non-negative. We can write for a general, Hermitian matrix \mathbf{P} that $\vec{v}^\dagger \mathbf{P} \vec{v} = e \geq 0$, where \vec{v} is the normalized eigenvector to the minimal eigenvalue e of \mathbf{P} . Suppose we sample the matrix $\mathbf{P} = \bar{\mathbf{P}} \pm \sigma(\mathbf{P})$. Then we can compute the eigenvector \vec{v} to the minimal eigenvalue \bar{e} of $\bar{\mathbf{P}}$ —with $\bar{e} = \vec{v}^\dagger \bar{\mathbf{P}} \vec{v}$ —and we also get the linearly propagated error from $\sigma(e) = |\vec{v}|^T \sigma(\mathbf{P}) |\vec{v}|$ with $|\vec{v}| = (|v_1|, |v_2|, \dots)^T$ [51].

In addition, let us also consider \mathbf{P}_n . That is the n th principal leading submatrix of \mathbf{P} . Consequently, we can estimate the minimal eigenvalues, $e_n = \bar{e}_n \pm \sigma(e_n)$. In order to provide statistical significance of the reconstructed matrix, we define the higher-order significances of the minimal eigenvalues of NQP matrix as follows:

$$\Sigma_n = \frac{\bar{e}_n}{\sigma(e_n)}. \quad (\text{A10})$$

As the minimal bound for the eigenvalues of classical states is $e_{\text{cl}} = 0$, the absolute value of the significance corresponds to the distance of e to e_{cl} in units of the error $\sigma(e)$, i.e., $|\Sigma_n| = |e - e_{\text{cl}}|/\sigma(e)$. The sign of Σ_n shows if we are consistent with this bound, $\Sigma_n \geq 0$, or clearly violate it.

4. Pattern functions for a discrete set of phases

Ideally, the phases at which the quadratures are measured should be scanned in the whole interval $0 \leq \varphi < \pi$ in a uniform distribution. In our actual experiment, the quadratures are obtain just at a given number I of fixed, equidistant phases. When the sampling function varies rapidly with respect to the phase as in the CV scenario, one can modify the pattern functions [37]. This reads

$$\begin{aligned} \bar{F} &= \int_{-\infty}^{\infty} dx \int_0^{\pi} d\varphi \frac{p(x; \varphi)}{\pi} f(x, \varphi) \\ &= \sum_{k=1}^I \int_{-\infty}^{\infty} dx \int_{-\frac{\pi}{2I}}^{\frac{\pi}{2I}} d\varphi \frac{p(x; \varphi_k + \varphi)}{\pi} f(x, \varphi_k + \varphi) \\ &\approx \sum_{k=1}^I \int_{-\infty}^{\infty} dx \frac{p(x; \varphi_k)}{\pi} \int_{-\frac{\pi}{2I}}^{\frac{\pi}{2I}} d\varphi f(x, \varphi_k + \varphi) \\ &= \frac{1}{I} \sum_{k=1}^I \int_{-\infty}^{\infty} dx p(x; \varphi_k) f'(x, \varphi_k), \end{aligned}$$

with the modified pattern function

$$f'(x, \varphi_k) = \frac{I}{\pi} \int_{-\frac{\pi}{2I}}^{\frac{\pi}{2I}} d\varphi f(x, \varphi_k + \varphi). \quad (\text{A11})$$

Appendix B: Weighted Sampling

In our scenario, we commonly have sets of data for equidistant, but not uniformly distributed phases; see Fig. 4. Then the ordinary arithmetic mean for the sampling does not give the correct estimation of the given physical quantities. For this reason, we will apply a weighted sampling approach to correct for the unbalanced distribution of data points. The general approach of weighted arithmetic means can be found, e.g., in Ref. [54]. Let us recall that for a data set $\{(x_j, \varphi_j)\}_{j=1, \dots, N}$, the considered weights ϖ_j ($\varpi_j \geq 0$ and $\sum_{j=1}^N \varpi_j = 1$) yield the sampling formula

$$\bar{F} = \sum_{j=1}^N \varpi_j f(x_j, \varphi_j). \quad (\text{B1})$$

In particular for $\varpi_j = 1/N$, we retrieve the unweighted case in Sec. A.

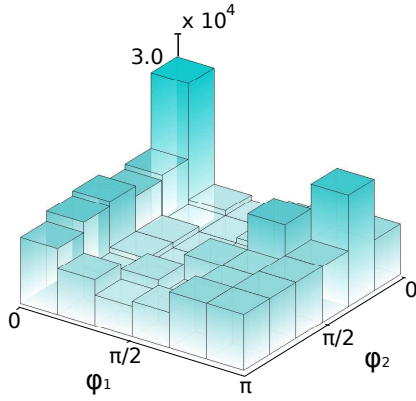


FIG. 4. The measured counts of the phases for the discrete-variable (DV) mode, φ_1 , and the continuous-variable (CV) mode, φ_2 . Our $N = 372000$ data points are non-uniformly distributed over $I = 6 \times 6 = 36$ phase intervals.

1. Single-mode case

Suppose we have a set of measured data points which is organized in the form $\{(x_j^{(l)}, \varphi^{(l)})\}_{j=1, \dots, N_l; l=1, \dots, I}$, where I is the number of measured phases and N_l is the number of measured quadratures for the l th phase. Without a loss of generality, we can assume that the data are ordered with increasing phase, $0 \leq \varphi^{(l)} < \varphi^{(l+1)} < \pi$. Interpreting a sampling formula in terms of a frequentist probability, we can estimate

$$F = \int_0^\pi d\varphi \int_{-\infty}^\infty dx \frac{p(x; \varphi)}{\pi} f(x, \varphi) \approx \bar{F} = \sum_{l=1}^I \sum_{j=1}^{N_l} \varpi_j^{(l)} f(x_j^{(l)}, \varphi^{(l)}), \quad (\text{B2})$$

where the weightings, $\varpi_j^{(l)} \geq 0$ and $\sum_{l,j} \varpi_j^{(l)} = 1$, represent the probability distribution $p(x; \varphi)$ in some limit. We define the Heaviside function $\Theta(t) = 1$ for $t \geq 0$ and $\Theta(t) = 0$ for $t < 0$. Further note that the probabilities are completely characterized by their cumulative distribution,

$$\mathcal{P}(x \leq X \wedge \varphi \leq \Phi) = \int_0^\Phi d\varphi \int_{-\infty}^X dx \frac{p(x; \varphi)}{\pi} \approx \sum_{l=1}^I \sum_{j=1}^{N_l} \varpi_j^{(l)} \Theta(X - x_j^{(l)}) \Theta(\Phi - \varphi^{(l)}). \quad (\text{B3})$$

In the following, we determine the coefficients $\varpi_j^{(l)}$ for the weighted sampling formula (B2) from the cumulative distribution \mathcal{P} in Eq. (B3). We need to satisfy the following two requirements: (i) The quadrature density $p(x; \varphi^{(l)})$ for a given phase is approximated by the relative frequencies of measurement outcomes $x_j^{(l)}$ for this phase $\varphi^{(l)}$; (ii) The recovered quadrature distribution of phases is uniformly distributed.

For (i), we consider the conditional probability

$$\mathcal{P}(x \leq X | \varphi = \varphi^{(l)}) = \frac{\mathcal{P}(x \leq X \wedge \varphi = \varphi^{(l)})}{\mathcal{P}(\varphi = \varphi^{(l)})}. \quad (\text{B4})$$

We get from our estimation on the one hand

$$\begin{aligned} \mathcal{P}(x \leq X | \varphi = \varphi^{(l)}) &= \frac{\int_{-\infty}^X dx \frac{p(x; \varphi^{(l)})}{\pi}}{\int_{-\infty}^\infty dx \frac{p(x; \varphi^{(l)})}{\pi}} \\ &= \int_{-\infty}^X dx p(x; \varphi^{(l)}) \approx \frac{1}{N_l} \sum_{j=1}^{N_l} \Theta(X - x_j^{(l)}), \end{aligned}$$

i.e., the normalized sum of all data points $x_j^{(l)}$ below X , and on the other hand

$$\mathcal{P}(x \leq X | \varphi = \varphi^{(l)}) \approx \frac{\sum_{j=1}^{N_l} \varpi_j^{(l)} \Theta(X - x_j^{(l)})}{\sum_{j=1}^{N_l} \varpi_j^{(l)}}.$$

This means that $\sum_j \Theta(X - x_j^{(l)})$ is proportional to $\sum_j \varpi_j^{(l)} \Theta(X - x_j^{(l)})$. As this relation holds for all X , we get that $\varpi_j^{(l)}$ has to be constant with respect to j ,

$$\varpi_j^{(l)} = \varpi^{(l)}. \quad (\text{B5})$$

Addressing requirement (ii), we consider a marginal phase distribution $\mathcal{P}(\varphi^{(l)} \leq \varphi < \varphi^{(l+1)})$ for phases in an interval, which is described by

$$\begin{aligned} \mathcal{P}(\varphi^{(l)} \leq \varphi < \varphi^{(l+1)}) &= \int_{\varphi^{(l)}}^{\varphi^{(l+1)}} d\varphi \int_{-\infty}^\infty dx \frac{p(x; \varphi)}{\pi} = \frac{\varphi^{(l+1)} - \varphi^{(l)}}{\pi} \end{aligned}$$

or estimated via

$$\mathcal{P}(\varphi^{(l)} \leq \varphi < \varphi^{(l+1)}) \approx \sum_{j=1}^{N_l} \varpi^{(l)} = \varpi^{(l)} N_l.$$

Hence, we conclude

$$\varpi^{(l)} = \frac{\varphi^{(l+1)} - \varphi^{(l)}}{N_l \pi}. \quad (\text{B6})$$

In our case, the phases are equidistant. That is, the interval from 0 to π is split into I equally sized intervals which results in $\varphi^{(l+1)} - \varphi^{(l)} = \pi/I$. Thus, we find for our measurements that the weighting coefficients for the sampling formula (B2) are

$$\varpi_j^{(l)} = \frac{1}{N_l I}. \quad (\text{B7})$$

2. Bipartite hybrid sampling

For our particular case of a bipartite system, we get the following sampling formula of discrete phases that

are not uniformly distributed:

$$\overline{P_{\Omega;m,n}(\alpha)} = \sum_{l=1}^I \sum_{j=1}^{N_l} \frac{1}{IN_l} g_j^{(l)}, \quad (\text{B8})$$

where we use

$$g_j^{(l)} = f'_{\Omega}(x_{1,j}^{(l)}, \varphi_1^{(l)}; \alpha, w) F'_{m,n}(x_{2,j}^{(l)}, \varphi_2^{(l)}) \quad (\text{B9})$$

and $\{(x_{1,j}^{(l)}, \varphi_1^{(l)}, x_{2,j}^{(l)}, \varphi_2^{(l)})\}_{j=1,\dots,N_l;l=1,\dots,I}$ defines our two-mode data set. It is worth mentioning that the total number of data points is $N = \sum_{l=1}^I N_l$. Here, instead of each of the data points contributing equally to the final average, we have a weighted mean of the product $g_j^{(l)}$ of pattern functions per phases pair. In Fig. 4, we showed the corresponding distribution of data points in the two-dimensional phase intervals which yields the weightings in Eq. (B7). Let us also stress that the pattern functions are independent of our weighting coefficients, cf. Eq. (B1). Further and as it was similarly shown in the

previous subsection, Eq. (B8) represents a proper estimate which satisfies our requirements (i) and (ii).

In the following, we derive the sampling-error estimation for the expression (B8). The standard approach is the treatment of all $g_j^{(l)}$ as random variables which are independent and distributed according to a normal distributions with a variance $\sigma(g_j^{(l)})^2$. This gives

$$\sigma(P_{\Omega;m,n}(\alpha))^2 = \sum_{l=1}^I \sum_{j=1}^{N_l} \left(\frac{1}{IN_l} \right)^2 \sigma_j^{(l)2}.$$

For a fixed phase $\varphi^{(l)}$, the random variables $g_j^{(l)}$ are identically distributed ($\sigma_j^{(l)} = \sigma^{(l)}$) which allows us to rewrite

$$\sigma(P_{\Omega;m,n}(\alpha))^2 = \frac{1}{I^2} \sum_{l=1}^I \frac{\sigma^{(l)2}}{N_l}, \quad (\text{B10})$$

where the empirical variance for a fixed phase is the standard estimate $\sigma^{(l)2} = \sum_{j=1}^{N_l} g_j^{(l)2} / N_l - (\sum_{j=1}^{N_l} g_j^{(l)} / N_l)^2$. Equation (B10) is the sampling error for the expression in Eq. (B8) for a non-uniform distribution of phases.

-
- [1] M. D. Reid, P. D. Drummond, W. P. Bowen, E. G. Cavalcanti, P. K. Lam, H. A. Bachor, U. L. Andersen, and G. Leuchs, The Einstein-Podolsky-Rosen paradox: From concepts to applications, *Rev. Mod. Phys.* **81**, 1727 (2009).
 - [2] B. Hensen *et al.*, Loophole-free Bell inequality violation using electron spins separated by 1.3 kilometres, *Nature (London)* **526**, 682 (2015).
 - [3] IBM Quantum Experience, <http://www.research.ibm.com/quantum>.
 - [4] D. Alsina and J. I. Latorre, Experimental test of Mermin inequalities on a five-qubit quantum computer, *Phys. Rev. A* **94**, 012314 (2016).
 - [5] M. Hebenstreit, D. Alsina, J. I. Latorre, B. Kraus, Compressed quantum computation using the IBM Quantum Experience, [arXiv:1701.02970 \[quant-ph\]](https://arxiv.org/abs/1701.02970).
 - [6] V. Scarani, H. Bechmann-Pasquinucci, N. J. Cerf, M. Dušek, N. Lütkenhaus, and M. Peev, The security of practical quantum key distribution, *Rev. Mod. Phys.* **81**, 1301 (2009).
 - [7] N. Gisin and R. Thew, Quantum communication, *Nat. Photon.* **1**, 165 (2007).
 - [8] R. J. Glauber, Coherent and Incoherent States of the Radiation Field, *Phys. Rev.* **131**, 2766 (1963).
 - [9] E. C. G. Sudarshan, Equivalence of Semiclassical and Quantum Mechanical Descriptions of Statistical Light Beams, *Phys. Rev. Lett.* **10**, 277 (1963).
 - [10] U. M. Titulaer and R. J. Glauber, Correlation Functions for Coherent Fields, *Phys. Rev.* **140**, B676 (1965).
 - [11] R. W. Spekkens, Negativity and Contextuality are Equivalent Notions of Nonclassicality, *Phys. Rev. Lett.* **101**, 020401 (2008).
 - [12] C. Ferrie and J. Emerson, Framed Hilbert space: Hanging the quasi-probability pictures of quantum theory, *New J. Phys.* **11**, 063040 (2009).
 - [13] H. Zhu, Quasiprobability representations of quantum mechanics with minimal negativity, [arXiv:1604.06974 \[quant-ph\]](https://arxiv.org/abs/1604.06974).
 - [14] J. Sperling, Characterizing maximally singular phase-space distributions, *Phys. Rev. A* **94**, 013814 (2016).
 - [15] K. E. Cahill and R. J. Glauber, Ordered Expansions in Boson Amplitude Operators, *Phys. Rev.* **177**, 1857 (1969).
 - [16] K. E. Cahill and R. J. Glauber, Density Operators and Quasiprobability Distributions, *Phys. Rev.* **177**, 1882 (1969).
 - [17] T. Kiesel and W. Vogel, Nonclassicality filters and quasiprobabilities, *Phys. Rev. A* **82**, 032107 (2010).
 - [18] E. Agudelo, J. Sperling, and W. Vogel, Quasiprobabilities for multipartite quantum correlations of light, *Phys. Rev. A* **87**, 033811 (2013).
 - [19] W. Vogel and D.-G. Welsch, *Quantum Optics* (Wiley-VCH Verlag GmbH & Co. KGaA, 2006).
 - [20] M. Malik, M. Mirhosseini, M. P. J. Lavery, J. Leach, M. J. Padgett, and R. W. Boyd, Direct measurement of a 27-dimensional orbital-angular-momentum state vector, *Nat. Commun.* **5**, 3115 (2014).
 - [21] N. Bent, H. Qassim, A. A. Tahir, D. Sych, G. Leuchs, L. L. Sánchez-Soto, E. Karimi, and R. W. Boyd, Experimental Realization of Quantum Tomography of Photonic Qudits via Symmetric Informationally Complete Positive Operator-Valued Measures, *Phys. Rev. X* **5**, 041006 (2015).
 - [22] J. S. Neergaard-Nielsen, M. Takeuchi, K. Wakui, H. Takahashi, K. Hayasaka, M. Takeoka, and M. Sasaki, Optical Continuous-Variable Qubit, *Phys. Rev. Lett.* **105**, 053602 (2010).
 - [23] A. S. Coelho, L. S. Costanzo, A. Zavatta, C. Hughes, M.

- S. Kim, and M. Bellini, Universal Continuous-Variable State Orthogonalizer and Qubit Generator, *Phys. Rev. Lett.* **116**, 110501 (2016).
- [24] S. Wallentowitz, R. L. de Matos Filho, and W. Vogel, Determination of entangled quantum states of a trapped atom, *Phys. Rev. A* **56**, 1205 (1997).
- [25] C. Monroe, D. M. Meekhof, B. E. King, and D. J. Wineland, A “Schrödinger Cat” Superposition State of an Atom, *Science* **272**, 1131 (1996).
- [26] M. Brune, E. Hagley, J. Dreyer, X. Maître, A. Maali, C. Wunderlich, J. M. Raimond, and S. Haroche, Observing the Progressive Decoherence of the “Meter” in a Quantum Measurement, *Phys. Rev. Lett.* **77**, 4887 (1996).
- [27] H. Jeong, A. Zavatta, M. Kang, S.-W. Lee, L. S. Costanzo, S. Grandi, T. C. Ralph, and M. Bellini, Generation of hybrid entanglement of light, *Nat. Photon.* **8**, 564 (2014).
- [28] O. Morin, K. Huang, J. Liu, H. Le Jeannic, C. Fabre, and J. Laurat, Remote creation of hybrid entanglement between particle-like and wave-like optical qubits, *Nat. Photon.* **8**, 570 (2014).
- [29] L. S. Costanzo, A. Zavatta, S. Grandi, M. Bellini, H. Jeong, M. Kang, S.-W. Lee, and T. C. Ralph, Properties of hybrid entanglement between discrete- and continuous-variable states of light, *Phys. Scr.* **90**, 074045 (2015).
- [30] P. van Loock, Optical hybrid approaches to quantum information, *Laser Photon. Rev.* **5**, 167 (2011).
- [31] U. L. Andersen, J. S. Neergaard-Nielsen, P. van Loock, and A. Furusawa, Hybrid discrete- and continuous-variable quantum information, *Nat. Phys.* **11**, 713 (2015).
- [32] H. Kwon and H. Jeong, Violation of the Bell-Clauser-Horne-Shimony-Holt inequality using imperfect photodetectors with optical hybrid states, *Phys. Rev. A* **88**, 052127 (2013).
- [33] S.-W. Lee and H. Jeong, Near-deterministic quantum teleportation and resource-efficient quantum computation using linear optics and hybrid qubits, *Phys. Rev. A* **87**, 022326 (2013).
- [34] C. H. Bennett, G. Brassard, C. Crépeau, R. Jozsa, A. Peres, and W. K. Wootters, Teleporting an unknown quantum state via dual classical and Einstein-Podolsky-Rosen channels, *Phys. Rev. Lett.* **70**, 1895 (1993).
- [35] J. Sperling, T. J. Bartley, G. Donati, M. Barbieri, X.-M. Jin, A. Datta, W. Vogel, and I. A. Walmsley, Quantum Correlations from the Conditional Statistics of Incomplete Data, *Phys. Rev. Lett.* **117**, 083601 (2016).
- [36] T. Kiesel, W. Vogel, M. Bellini, and A. Zavatta, Nonclassicality quasiprobability of single-photon-added thermal states, *Phys. Rev. A* **83**, 032116 (2011).
- [37] T. Kiesel, W. Vogel, B. Hage, and R. Schnabel, Direct Sampling of Negative Quasiprobabilities of a Squeezed State, *Phys. Rev. Lett.* **107**, 113604 (2011).
- [38] U. Leonhardt, H. Paul, and G. M. D’Ariano, Tomographic reconstruction of the density matrix via pattern functions, *Phys. Rev. A* **52**, 4899 (1995).
- [39] Th. Richter, Determination of field correlation functions from measured quadrature component distributions, *Phys. Rev. A* **53**, 1197 (1996).
- [40] A. I. Lvovsky and M. G. Raymer, Continuous-variable optical quantum-state tomography, *Rev. Mod. Phys.* **81**, 299 (2009).
- [41] S. Grandi, A. Zavatta, M. Bellini, and M. G. A. Paris, Experimental quantum tomography of a homodyne detector, [arXiv:1505.03297 \[quant-ph\]](https://arxiv.org/abs/1505.03297).
- [42] M. Gunawardena and D. S. Elliott, Atomic Homodyne Detection of Weak Atomic Transitions, *Phys. Rev. Lett.* **98**, 043001 (2007).
- [43] C. Gross, H. Strobel, E. Nicklas, T. Zibold, N. Bargill, G. Kurizki, and M. K. Oberthaler, Atomic homodyne detection of continuous-variable entangled twin-atom states, *Nature (London)* **480**, 219 (2011).
- [44] E. Verhagen, S. Deeglise, S. Weis, A. Schliesser, and T. J. Kippenberg, Quantum-coherent coupling of a mechanical oscillator to an optical cavity mode, *Nature (London)* **482**, 63 (2012).
- [45] G. M. D’Ariano, U. Leonhardt, and H. Paul, Homodyne detection of the density matrix of the radiation field, *Phys. Rev. A* **52**, R1801 (1995).
- [46] U. Leonhardt, M. Munroe, T. Kiss, Th. Richter, and M. G. Raymer, Sampling of photon statistics and density matrix using homodyne detection, *Opt. Commun.* **127**, 144 (1996).
- [47] Th. Richter, Pattern functions used in tomographic reconstruction of photon statistics revisited, *Phys. Lett. A* **211**, 327 (1996).
- [48] E. Agudelo, J. Sperling, W. Vogel, S. Köhnke, M. Mraz, and B. Hage, Continuous sampling of the squeezed-state nonclassicality, *Phys. Rev. A* **92**, 033837 (2015).
- [49] See the Supplemental Material for the reconstruction of the NQP matrix, which includes the Refs. [37, 39, 51–54].
- [50] J. Sperling, W. Vogel, and G. S. Agarwal, Quantum state engineering by click counting, *Phys. Rev. A* **89**, 043829 (2014).
- [51] J. Sperling, M. Bohmann, W. Vogel, G. Harder, B. Brecht, V. Ansari, and C. Silberhorn, Uncovering Quantum Correlations with Time-Multiplexed Click Detection, *Phys. Rev. Lett.* **115**, 023601 (2015).
- [52] Th. Richter, Direct sampling of density matrix in displaced Fock-state basis from quadrature distributions and reconstruction of quasiprobability distributions, *J. Mod. Opt.* **46**, 1167 (1999).
- [53] I. S. Gradshteyn and I. M. Ryzhik, *Table of Integrals, Series, and Products*, 7th ed. (Academic Press, Cambridge, MA, 2007).
- [54] P. R. Bevington, *Data Reduction and Error Analysis for the Physical Sciences* (McGraw-Hill, New York, N.Y., 1969).